

Dynamical Approach to Analytic Continuation of Quantum Monte Carlo Data

Mark Jarrell and Ofer Biham

Department of Physics, The Ohio State University, Columbus, Ohio 43210

(Received 7 July 1989)

A new method of analytic continuation from a Matsubara single-particle Green's function to a spectral function is presented. We recast this problem onto a new one where we dynamically minimize a suitably defined potential. Our method allows the imposition of physical constraints such as smoothness and adherence to the sum rule. The method is applied to the symmetric Anderson impurity model. We show how the spectral function changes with the Kondo temperature T_K , the hybridization width Δ , and the Coulomb potential U .

PACS numbers: 71.10.+x, 71.55.-i

In recent years various advances have been made in the area of quantum Monte Carlo simulations.¹⁻³ These methods allow one to directly determine the static, but not the dynamic, properties of the systems being simulated. The reason is that the Monte Carlo simulation provides data along the imaginary-time direction, while to understand the dynamic properties the imaginary-time data must be analytically continued to the real axis.

Thus, a reliable method to analytically continue a single-particle Green's function tabulated at imaginary Matsubara frequencies to a spectral function of real frequencies is needed. Previously, analytic continuation has been approached either by Padé approximation⁴ or by least-squares fitting.⁵ The Padé method suffered from sensitivity to noise in the data and the accumulation of round-off errors due to the finite precision of the computer. The least-squares method was less sensitive to these problems; however, it provided results which were only qualitatively correct.⁵

In this Letter we present a new technique of analytic continuation. We demonstrate that analytic continuation from the imaginary-frequency Green's function to the real-frequency spectral function is equivalent to the minimization of a suitably defined potential.

We find this potential, and then introduce an artificial dynamics which flows towards the minimum of this potential. This process is insensitive to the accumulation of round-off error and to moderate amounts of noise in the data. We chose a dynamical approach since it allows us to impose physical constraints on the resulting spectral function in a nonlinear way. In particular, we enforce the spectral density sum rule and uniform positivity as nonlinear constraints. We also impose a linear constraint that eliminates wild fluctuations which can result from noisy data.

We have successfully applied this method to the symmetric Anderson model. However, to demonstrate the usefulness of this approach, we first present the results for a toy model with features similar to those of the Anderson model. The spectral function of this toy model is composed of a central peak and two side peaks (Fig. 1). For the toy model the single-particle Green's function of

imaginary Matsubara frequencies can be calculated exactly. The resulting data, with noise added, are analytically continued to a spectral function of real frequencies. The resolution of this method is demonstrated in Fig. 1. Note that the essential features are relatively unaffected by as much as 10% added noise.

In Figs. 2 and 3 we present the spectral function of the symmetric Anderson model. The Matsubara-frequency data were obtained from a determinantal Monte Carlo algorithm developed by Hirsch and Fye.¹ In Fig. 2, the symmetric-Anderson-model spectral function for $T=0.025$, $U=6.0$, and several different T_K 's is presented. Note that the central peak becomes higher and narrower as T_K increases. In Fig. 3, the symmetric-Anderson-model spectral function for $T_K=0.02$ and two different values of U is presented. Note that the side peak is centered roughly at $U/2$.

Our method is based upon the spectral representation of the Green's function,

$$G(iv_n) = \int_{-\infty}^{\infty} \frac{A(\omega)}{iv_n - \omega} d\omega. \quad (1)$$

Here, $G(iv_n)$ is a single-particle Green's function, $v_n = (2n+1)\pi T$, and $A(\omega)$ is the corresponding spectral function. We discretize the spectral function by expanding it as a series of δ functions, $A(\omega) = \sum_{m=-\infty}^{\infty} A_m \times \delta(\omega - \omega_m)$, and choose the real frequencies on a regular grid of spacing $\Delta\omega$. In this paper we concentrate on the particle-hole symmetric case where $A(\omega) = A(-\omega)$, although the method applies to the nonsymmetric case as well. For the particle-hole symmetric case, where $\text{Re}G(iv_n) = 0$, Eq. (1) reduces to

$$\frac{\text{Im}G(iv_n)}{v_n} = - \sum_{m=-\infty}^{\infty} \frac{A_m}{\omega_m^2 + v_n^2}, \quad n=0, \pm 1, \pm 2, \dots \quad (2)$$

In order to find the spectral function, we consider $\{A_p\}$ as a set of dynamical variables evolving in an artificial time t . This dynamics evolves towards the minimum of a potential where the $\{A_p\}$ are the solution to Eq. (2). In order to define this potential we take the real-frequency grid to be the same as the imaginary-frequency grid, i.e.,

$\omega_n = v_n$. The potential then takes the form⁶

$$V(\{A_p\}) = V_1(\{A_p\}) + V_2(\{A_p\}), \quad (3)$$

where

$$V_1(\{A_p\}) = \sum_n \frac{\text{Im}G(iv_n)}{v_n} A_n + \frac{1}{2} \sum_{n,m} \frac{A_n A_m}{\omega_m^2 + v_n^2}, \quad (4)$$

and

$$V_2(\{A_p\}) = C_S \left[\sum_n A_n - 1 \right]^p + C_G \sum_n (A_{n-1} - 2A_n + A_{n+1})^2 / (\Delta\omega)^4. \quad (5)$$

The term $V_1(\{A_p\})$ is constructed such that minimizing it is equivalent to solving Eq. (2). $V_1(\{A_p\})$ is a quadratic potential in an infinite-dimensional space of $\{A_p\}$ which has a unique minimum.⁷ In some directions this minimum can be very shallow; therefore, any deviation of A_n in these directions will barely change the po-

tential. Therefore, an equivalent small change in the $G(iv_n)$ data can cause a large change in $A(\omega)$; thus, the difficulty in obtaining the spectral function A .

The first term in $V_2(\{A_p\})$ is constructed such that minimizing it will impose the sum-rule constraint $\int_{-\infty}^{\infty} A(\omega) d\omega = 1$, while the second, Ginzburg-type, term inhibits spurious fluctuations of A due to noisy data by making discontinuities in $A(\omega)$, or its derivative, energetically unfavorable. The exponent p can be any even power, and C_S and C_G are chosen so that once these two constraints are imposed, $V_2(\{A_p\})$ is negligible, and $V_1(\{A_p\})$ dominates. In addition, we do not allow any of the set $\{A_p\}$ to become negative. This amounts to the addition of a set of barrier potentials which become infinite if any of the $\{A_p\}$ become negative.

The force conjugate to A_n is $f_n = -\partial V(\{A_p\})/\partial A_n$. Our dynamics corresponds to a system of massless particles with dissipation. Thus, the dynamical equations of motion are

$$-\frac{\partial A_n}{\partial t} = \frac{\text{Im}G(iv_n)}{v_n} + \sum_{m=-\infty}^{\infty} \frac{A_m}{\omega_m^2 + v_n^2} + 4C_S \left(\sum_m A_m - 1 \right)^{p-1} + \frac{2C_G (A_{n-2} - 4A_{n-1} + 6A_n - 4A_{n+1} + A_{n+2})}{(\Delta\omega)^4}. \quad (6)$$

We integrate these equations from $t=0$ until they converge to a fixed point, where $\partial A_n/\partial t = 0$. Then the resulting set $\{A_p\}$ defines the desired spectral function.

One can also choose the real-frequency grid to be different from the imaginary-frequency grid. In this case it is not possible to define a potential; however, we find that the dynamical equations (6) still flow to a single fixed point, and this corresponds to the proper solution of the analytic continuation. This is a unique property of our dynamical approach. It allows us to find the spectral function even when a potential does not exist. Since the real-frequency grid can be chosen arbitrarily, we can make it finer in regions which need better resolution. However, in this paper we do not use this option.

In practice, we consider only a finite number L of equations according to the number of points at which $G(iv_n)$ is evaluated. The real-frequency grid is chosen such that it will have the same number of points L and still include the region of interest. Initial values of A_n can be chosen with some arbitrariness so long as they are not too large. However, we find it best to choose them so that they are all equal and satisfy the sum rule. For p , the exponent of the sum-rule constraint, we found that all even powers between 2 and 6 work well; however, we found 4 to work best in that it allowed the imposition of the sum rule to almost arbitrary accuracy with negligible residual forces. The parameters C_S and C_G are increased from zero until the sum rule is satisfied and smoothness is obtained. In addition to imposing the constraints, these terms make the net potential less shallow, resulting in faster convergence to the minimum. Typical values of these parameters for the Monte Carlo data are $C_S = 0.03$ and $C_G = 0.001$. We find that further small increases of C_S and C_G do not change the results. We then

solve the set of dynamical equations (6) using a standard method such as fourth-order Runge-Kutta until all forces become smaller than some predetermined parameter $\epsilon \approx 10^{-5}$, which must be smaller than the measured error in $G(iv_n)$.

The convergence is fast. Generally, for a set of sixty Matsubara frequencies, convergence takes about one minute on a VAX 8600 with single precision. After convergence is obtained, one must examine the contributions of the forces associated with the V_2 term, and make sure that they are smaller than the error bars of the Monte Carlo $G(iv_n)$. We always found this to be the case. One can consider these contributions as a correction to the Monte Carlo data. In the toy model discussed below, we found that the residual forces due to V_2 tended to correct for the random error introduced into the data.

We first apply this method to a toy problem where the spectral function is composed of three squared Lorentzian peaks.⁸ One peak is located at the origin with weight 0.55 and width 0.5, and the other peaks are located symmetrically away from the origin at $\omega = \pm 2.0$, with weights 0.225 and widths 0.5. For this model, $G(iv_n)$ can be obtained explicitly. In order to imitate the way Monte Carlo data are processed, we Fourier transform $G(iv_n)$ to $G(\tau)$, where τ is defined on a grid from 0 to $\beta = 1/T$, $T = 0.02$, of width $\Delta\tau = 0.25$, such that $L\Delta\tau = \beta$. We then Fourier transform this discrete data to the first L Matsubara frequencies. We then add noise to $G(iv_n)$ by multiplying each datum by $1 + 2C_{\text{noise}}(R - \frac{1}{2})$, where R is a random number between 0 and 1. In Fig. 1 we present the exact spectral function (solid line) along with those for $C_{\text{noise}} = 0.02$ (dashed line), 0.05 (dotted line), and 0.10 (dot-dashed line). The important feature is

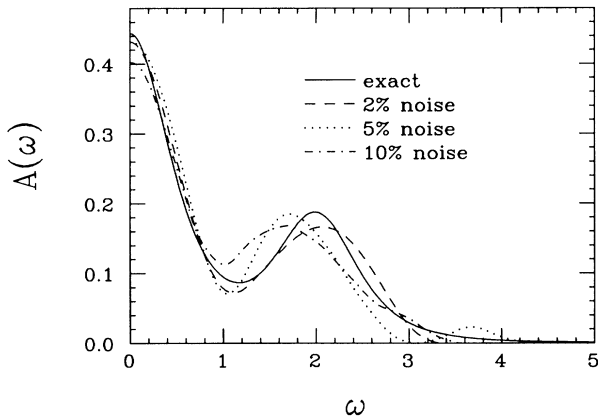


FIG. 1. Comparison of exact and analytically continued results. The exact result (solid line) consists of three squared Lorentzian peaks (Ref. 8), one centered at the origin with weight 0.55 and width 0.5, and the other two at $\omega = \pm 2.0$, with weights 0.225 and widths 0.5. Only positive frequencies are plotted since the data are symmetric. The data were processed to imitate Monte Carlo data with $\Delta\tau=0.25$ and $T=0.02$. The analytically continued data have 2%, 5%, and 10% random noise added (dashed, dotted, and dot-dashed lines, respectively).

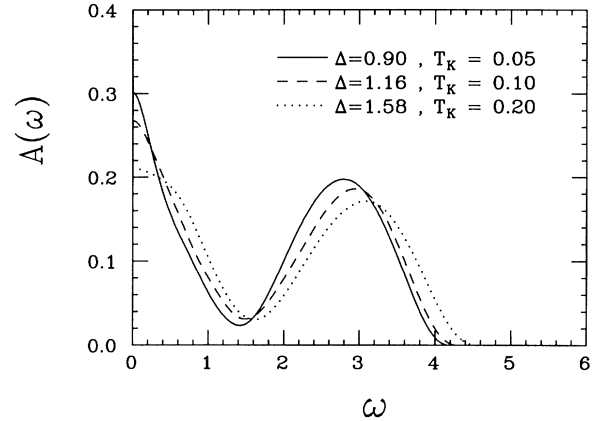


FIG. 2. Spectral density function for the symmetric Anderson model when $U=6.0$ and $T=0.025$ for various values of Δ and the corresponding T_K 's when $\Delta\tau=0.25$. Note that the central peak width grows with T_K , and the height grows with $1/\Delta$. This behavior is expected in the limit $T/T_K \rightarrow 0$ where the Friedel sum rule applies (Ref. 12). The side peaks shift towards the origin as the central peak becomes more pronounced (T_K becomes larger) as expected from perturbation theory (Ref. 13). We estimate the vertical statistical error bars to be ≈ 0.02 (Ref. 9).

that, while the side peaks change slightly, the central peak remains relatively unaffected.

We also found that, for a given temperature, the resolution of our calculation depends crucially upon $\Delta\tau = \beta/L$. For example, in this toy problem, we were able to resolve a central peak of width 0.5 when $\Delta\tau=0.25$. However, to resolve a sharper peak of width 0.1, for example, one should take $\Delta\tau$ to be smaller.

We applied this method to the symmetric Anderson model of magnetic impurities. We generate the Green's function of Matsubara frequencies using a quantum Monte Carlo algorithm discussed by Hirsch and Fye.¹ In this simulation the problem is cast into a discrete path-integral formalism in imaginary time, τ_l , where $\tau_l = l\Delta\tau$, $\Delta\tau = \beta/L$, and L is the number of time slices. At each measurement step we measure both $G(\tau_l)$ and the first L values of its discrete Fourier transform $G(iv_n)$. The standard deviation, and the systematic errors associated with the finite value of $\Delta\tau$, for $G(iv_n)$ were each estimated to be of order 1% for the data in Fig. 2 and 2% for Fig. 3.⁹

The Anderson model, in the limit of infinite metallic bandwidth, is characterized by a hybridization width $\Delta = \pi N(0)V^2$ [where V is the hybridization matrix element, and $N(0)$ is the density of states at the Fermi surface], an on-site repulsion U , and a Kondo temperature $T_K = 0.364(2\Delta U/\pi)^{1/2} e^{-\pi U/8\Delta}$.^{10,11} In Fig. 2 we show the spectral function of the symmetric Anderson model when $U=6.0$, $T=0.025$, and $\Delta\tau=0.25$ for various values of Δ and associated T_K 's. One expects that the

width of the central peak should be of order T_K , which is smaller than the resolution of our calculation at the given values of T and $\Delta\tau$. Nevertheless, note that the width of the central peak increases with T_K , and that the height increases with $1/\Delta$. This behavior is expected in the limit $T/T_K \rightarrow 0$ where the Friedel sum rule¹² applies. The side peak associated with the $f^1 \rightarrow f^2$ transition is located roughly at $\omega = U/2$ with width $\approx 2\Delta$, in accord with results from a $1/N$ expansion.¹⁴ The side

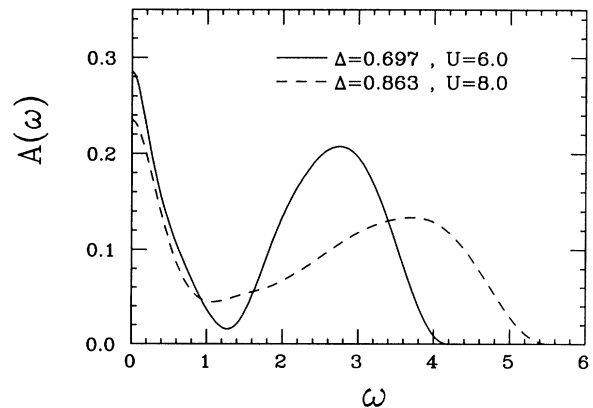


FIG. 3. Spectral density function for the symmetric Anderson model when $T_K=0.02$ and $T=0.025$ for two values of U and Δ when $\Delta\tau=0.25$. Note that the side peak is always located at roughly $U/2$ with width $\approx 2\Delta$. We estimate the vertical statistical error bars to be ≈ 0.03 (Ref. 9).

peaks shift away from the origin as the central peak becomes more pronounced (i.e., T_K becomes larger). This behavior is expected from perturbation theory.¹³ The location of the side peaks is illustrated further in Fig. 3. In this figure the spectral function is plotted when $T=0.025$ and $\Delta\tau=0.25$ for two different values of U and corresponding values of Δ chosen so that $T_K=0.02$. In each case the side peak is located at $\approx U/2$, and has width $\approx 2\Delta$.

In conclusion, we have presented a method of analytic continuation of a single-particle Green's function of Matsubara frequencies to a spectral function of real frequencies. The essential feature of our method is the equivalence of analytic continuation and the minimization of a potential. We minimize the potential by an iterative dynamic process constrained to produce a spectral function which is smooth and satisfies the sum rule. As a result, our method is less sensitive to noise than previous techniques, works over a wider temperature range, and is insensitive to the accumulation of error due to finite numerical precision of the computer.

While in the final stages of this work we received a paper from White *et al.*¹⁵ describing a similar method. The primary differences are that they directly analytically continue the imaginary-time Green's function⁵ with a weighted least-squares method.

We are pleased to acknowledge useful conversations with D. L. Cox, J. Deisz, C. Jayaprakash, H. R. Krishna-murthy, R. Mills, D. Sullivan, W. Wenzel, and J. W. Wilkins. This work was supported in part by the DOE, Basic Energy Science, Division of Materials Research, NSF Grant No. DMR8451911, and the Ohio Supercomputer Center.

¹J. E. Hirsch and R. M. Fye, Phys. Rev. Lett. **56**, 2521 (1986).

²S. Sorella *et al.*, in Proceedings of the Adriatico Research Conference 1988 (to be published).

³S. R. White, D. J. Scalapino, R. L. Sugar, E. Y. Loh, J. E. Gubernatis, and R. T. Scalettar, Phys. Rev. B **40**, 506 (1989).

⁴H. J. Vidberg and J. Serene, J. Low Temp. Phys. **29**, 179 (1977).

⁵H.-B. Schüttler and D. J. Scalapino, Phys. Rev. Lett. **55**, 1204 (1985).

⁶Note that $\omega_n = \nu_n$ and we treat them as numerically equivalent, although they still retain their different interpretation as points along the real and imaginary axes, respectively.

⁷Since V_1 is quadratic it has a single extremum. In order to show that this extremum is a minimum we applied Gundelfinger's determinantal rule; see, e.g., E. K. McLachlan, *Calculus of Several Variables* (Brooks/Cole, Belmont, CA, 1968). As the order of the matrices increases the determinants decrease exponentially to 0^+ , indicating that in some directions this minimum is very shallow.

⁸A square Lorentzian centered at ω_0 with width 0.64δ takes the form $(2\delta^3/\pi)/[(\omega - \omega_0)^2 + \delta^2]^2$.

⁹The statistical error in $A(\omega)$ can be estimated by analytically continuing independent sets of $G(iv_n)$, and calculating the variance of the resulting average $A(\omega)$.

¹⁰F. D. Haldane, J. Phys. C **11**, 5015 (1978).

¹¹H. R. Krishna-murthy, J. W. Wilkins, and K. G. Wilson, Phys. Rev. B **21**, 1003 (1979).

¹²D. C. Langreth, Phys. Rev. **150**, 516 (1966).

¹³B. Horvatic, D. Sokcevic, and V. Zlatic, Phys. Rev. B **36**, 675 (1987).

¹⁴N. E. Bickers, D. L. Cox, and J. W. Wilkins, Phys. Rev. B **36**, 2036 (1987).

¹⁵S. R. White, D. J. Scalapino, R. L. Sugar, and N. E. Bickers (to be published).